Original Article
An interspecies study of lipid profiles and atherosclerosis in familial hypercholesterolemia animal models with low-density lipoprotein receptor deficiency

Kunxiang He[1*], Jinjie Wang[1*], Haozhe Shi[1], Qiongyang Yu[1], Xin Zhang[2], Mengmeng Guo[1], Huijun Sun[3], Xiao Lin[1], Yue Wu[4], Luya Wang[4], Yuhui Wang[1], Xunde Xian[5], George Liu[1]

[1]Institute of Cardiovascular Sciences and Key Laboratory of Molecular Cardiovascular Sciences, Ministry of Education, Peking University, Beijing 100191, China; [2]Hebei Invivo Biotech Co, Shijiazhuang, China; [3]College of Pharmacy, Dalian Medical University, Dalian 116044, China; [4]The Key Laboratory of Remodeling-Related Cardiovascular Diseases, Ministry of Education, Beijing An Zhen Hospital Affiliated to Capital Medical University, Beijing Institute of Heart, Lung and Blood Vessel Diseases, Beijing 100029, China; [5]Department of Molecular Genetics, UT Southwestern Medical Center, Dallas 75390, Texas, USA. *Equal contributors.

Abstract: Small rodents, especially mice and rats, have been widely used in atherosclerosis studies even though humans exhibit completely different lipoprotein metabolism and atherosclerotic characteristics. Until recently, various rodent models of human familial hypercholesterolemia (FH) have been created, including mice, rats, and golden Syrian hamsters. Although hamsters reportedly possess metabolic features similar to humans, there is no systematic characterization of the properties of circulating lipids and atherosclerotic lesions in these rodent models. We used three FH animal species (mice, rats, and hamsters) with low-density lipoprotein receptor (Ldlr) deficiency to fully assess lipoprotein metabolism and atherosclerotic characteristics. Compared to chow diet-fed mice and rats, Ldlr knockout (KO) hamsters showed increased cholesterols in LDL fractions similar to human FH patients. Upon 12-week high-cholesterol/high-fat diet feeding, both heterozygous and homozygous Ldlr KO hamsters displayed hyperlipidemic phenotypes, whereas only homozygous Ldlr KO mice and rats showed only moderate increases in plasma lipid levels. Moreover, rats were resistant to diet-induced atherosclerosis compared to mice, and hamsters showed more atherosclerotic lesions in the aortas and coronary arteries. Further morphological study revealed that only hamsters developed atherosclerosis in the abdominal segments, which is highly similar to FH patients. This unique animal model will provide insight into the translational study of human atherosclerosis and could be useful for developing novel treatments for FH patients.

Keywords: Mouse, rat, hamster, low-density lipoprotein receptor, familial hypercholesterolemia, atherosclerosis

Introduction

Familial hypercholesterolemia (FH) is an autosomal-dominant inherited condition that causes very high levels of cholesterol in the blood, mainly low-density lipoprotein LDL cholesterol (LDL-C), which leads to an increased incidence of premature cardiovascular disease (CVD) [1]. Genetic studies have established the association of FH and variants in three genes: LDL receptor (LDLR), apolipoprotein B (APOB), and proprotein convertase subtilisin/kexin type 9 (PCSK9). Among these, loss-of-function mutations in LDLR account for approximately 90% of cases [1, 2].

Although the molecular mechanisms underlying FH pathogenesis have been extensively investigated using genetically manipulated small rodents like LDLR-deficient mice and rats, these species are not ideal FH models because of differences in lipoprotein metabolism among mice, rats, and humans [3, 4]. Mice and rats lack endogenous cholesteryl ester transfer protein (CETP) but have higher hepatic LDLR expression levels and display high ApoB editing activity in both the intestine and liver, which contribute to a circulating lipoprotein profile with elevated high-density lipoprotein (HDL) cholesterol (HDL-C), making these two species resistant to diet-induced hypercholesterolemia [5, 6]. Hy-

percholesterolemia can reportedly be induced in homozygous Ldlr-deficient mice by the Paigen diet containing 1.25% cholesterol and 0.5% cholate. However, this treatment elicits severe liver toxicity and leads to weight loss and sickness in mice, indicating the Paigen diet should be avoided in experimental animal studies [7, 8]. Moreover, FH is a genetic disease with a gene dosage-dependent effect. Homozygous and heterozygous FH patients show very high and moderately increased cholesterol levels in blood, respectively, but the risk of CVD is significantly increased in both groups. In contrast to FH patients, heterozygous Ldlr-deficient mice exhibit unexpectedly normal plasma cholesterol concentrations, suggesting that one copy of the *Ldlr* gene is sufficient to maintain normal plasma cholesterol levels in mice. Thus, heterozygous Ldlr KO mice have not been used to study hypercholesterolemia and atherosclerosis. Ldlr KO rats have also been generated and characterized [9, 10], but information on similarities of Ldlr KO rats and FH patients is still lacking, and it is unknown whether heterozygous Ldlr KO rats can mimic heterozygous FH.

Golden Syrian hamsters possess similar lipoprotein metabolism to humans [11-13], so we used the CRISPR/Cas9 system to generate a hamster model with Ldlr deficiency and found that Ldlr KO hamsters display hyperlipidemia and atherosclerosis like humans [14]. To better understand the similarities and differences of lipid profiles and atherosclerosis among three species with Ldlr deficiency, in the present study we used wild-type (WT), heterozygous, and homozygous animals in a systematical evaluation. Compared to mice and rats, both heterozygous and homozygous Ldlr KO hamsters replicate the phenotypes of hyperlipidemia and mimic the atherosclerotic plaque distribution observed in the aortic roots, coronary arteries, and abdominal segments of FH patients.

Materials and methods

Animals and diets

Ldlr KO hamsters were created with CRISPR/Cas9 in our lab as described previously [14]. WT and Ldlr KO rats were purchased from Gene Biotechnology Company (Beijing, China), and mice were obtained from the Experimental Animal Center of Peking University Health Science Center. All animals were housed under specific pathogen-free conditions with a 14:10-h light-dark cycle for hamsters and a 12:12-h light-dark cycle for mice and rats. Animals were fed either a regular chow diet (20% protein and 4% fat; Beijing Ke'ao company, Beijing, China) or a high-cholesterol/high-fat (HCHF) diet (0.5% cholesterol and 15% fat) for 12 weeks. Plasma was collected after overnight fasting. In our studies, male animals aged 10-12 weeks were used. All experiments were performed under the principle of experimental animal health (NIH released no. 85Y231996 Revision) and approved by the laboratory animal ethics committee of Peking University (LA2010-059).

Clinical characterization of FH patients

Plasma samples of six patients with familial hypercholesterolemia and three normal subjects (male, 0-40 years old) were gifts from An Zhen Hospital, Beijing. Patient diagnoses were made based on genetic analyses and clinical manifestations. The patients were divided into heterozygotes and homozygotes according *Ldlr* gene mutations [15, 16].

Analysis of plasma lipids, lipoproteins, and apolipoproteins in different species

Plasma ApoE, ApoB, and ApoA1 were detected by western blotting using methods described previously [17]. Briefly, 1 μL of plasma was subjected to 6% or 12% sodium dodecyl sulfate polyacrylamide gel electrophoresis for ApoB or ApoA1/ApoE, then transferred to a polyvinylidene fluoride membrane for immunoblotting with rabbit anti-ApoA1 (Calbiochem, San Diego, CA, USA), goat anti-ApoE (Calbiochem), or goat anti-ApoB (Calbiochem, California, USA) polyclonal antibody. Mouse anti-ApoB monoclonal antibody (Santa Cruz Biotechnology, Dallas, TX, USA), rabbit anti-ApoA1 (Santa Cruz Biotechnology), and goat anti-ApoE (Calbiochem) were used for human samples. Proteins were visualized by incubation with horseradish peroxidase-conjugated secondary antibodies, followed by enhanced chemiluminescence detection (Molecular Imager Gel Doc XR System, Bio-Rad, Hercules, CA, USA). Plasma total cholesterol (TC) and triglyceride (TG) were measured using enzymatic commercial kits (Sigma-Aldrich, St. Louis, MO, USA). Plasma lipoprotein profiles were analyzed by fast protein liquid chromatography (FPLC). Briefly, 200 μl of pooled plasma from each genotype was applied to Tricorn

high-performance Superose S-6 10/300 GL column (Amersham Biosciences, Little Chalfont, UK), and then eluted with phosphate-buffered saline (PBS) at a flow rate of 0.25 mL/min. Cholesterol contents in each fraction (500 µL/fraction) were determined by the same commercial kit.

Lipid extraction

Lipids were extracted according to modified method of Bligh and Dyer [18]. Briefly, 100 mg liver tissues were homogenized with 1 mL cold PBS. Then lipids were extracted by adding chloroform/methanol (v:v=2:1). Ten-milliliter glass tubes were used to avoid polymer contamination. Samples were vortexed for 2 min and then incubated for 20 min at room temperature, followed by centrifugation at 1000 rpm for 5 min. The chloroform layer was then transferred with a glass syringe and dried under nitrogen. Lipid samples were stored in -80°C freezer for future use. TC and TG contents were measured using enzymatic commercial kits (Sigma-Aldrich).

Pathological analysis

Animals were sacrificed at the indicated times following different diet interventions. Heart tissues and whole aortas were harvested after perfusion with 30 mL 0.01 M PBS and placed in 4% paraformaldehyde solution for 1 week, followed by an overnight incubation in 20% sucrose solution. The heart tissues were embedded in Optimal Cutting Temperature (OCT) compound and then cryo-sectioned (7-µm sections). The atherosclerotic plaques in aortic roots and whole aortas were analyzed with 0.3% Oil Red O (ORO) staining (Sigma-Aldrich). Coronary atherosclerosis was scored by the plaques containing fatty streaks and are expressed as the proportion of the total coronary arteries, which were normal (no plaque), <5% occluded, 5%-50% occluded, and >50% occluded.

For the analysis of atherosclerotic plaque components, CD68 and vascular cell adhesion protein 1 (VCAM-1) in macrophages and alpha-smooth muscle actin (α-SMA) in smooth muscle cells were stained with a CD68 antibody (ab-53444, diluted at 1:200; Abcam, Cambridge, UK), VCAM-1 antibody (ab134047, diluted at 1:200; Abcam) and α-SMA antibody (A5228, diluted at 1:200; Sigma-Aldrich), respectively. The slices were incubated with blocking solution (PBS containing 10% goat serum) for 30 min, then incubated with primary antibody overnight at 4°C and washed three times with PBS followed by an incubation with the appropriate biotinylated secondary antibodies (1:200, ABC Vectastain; Vector Laboratories, Burlingame, CA, USA) and visualized using 3.3'-diaminobenzidine (DAB; Vectastain, Vector Laboratories) [19].

For Sirius red staining, hepatic tissues were fixed with 4% paraformaldehyde solution overnight. Fixed liver tissues were embedded in paraffin and then cut into 4-µm sections and then stained with Picrosirius Red Stain kit (Polysciences, Inc., Warrington, PA). Briefly, slices were deparaffinized and washed with double distilled (DI) water, then stained in hematoxylin for 8 min and rinsed well in DI water. The slices were placed in solution A for 2 min and rinsed in DI water, followed by an incubation with solution B for 60 min and then solution C for 2 min. Next, 70% ethanol was applied to the slices for 45 s, and then samples were dehydrated to mount. For hematoxylin-eosin (HE) staining, samples were immersed in xylene and alcohol, then stained with hematoxylin for 5 min, followed by another incubation with eosin for 3 min. Afterward, slices were re-immersed in alcohol and xylene, and then mounted. Fatty liver severity was assessed by HE and Sirius red staining as previously defined [20].

Statistical analysis

Group comparisons were performed using two-way analysis of variance followed by Tukey's test. GraphPad Prism 7.0 software (GraphPad Software, La Jolla, CA, USA) was used for all statistical analyses. Differences at $P < 0.05$ were considered significant. All data are expressed as mean ± SEM.

Results

Plasma lipid profiles in FH patients and chow-fed Ldlr KO animals

To investigate plasma lipid and lipoprotein levels in different Ldlr KO animals and FH patients, we collected plasma from three normal subjects and six patients with FH (three heterozygotes [HeFH] and three homozygotes [HoFH]). On a regular chow diet, Ldlr-/- hamsters showed hypercholesterolemia with a TC concentration
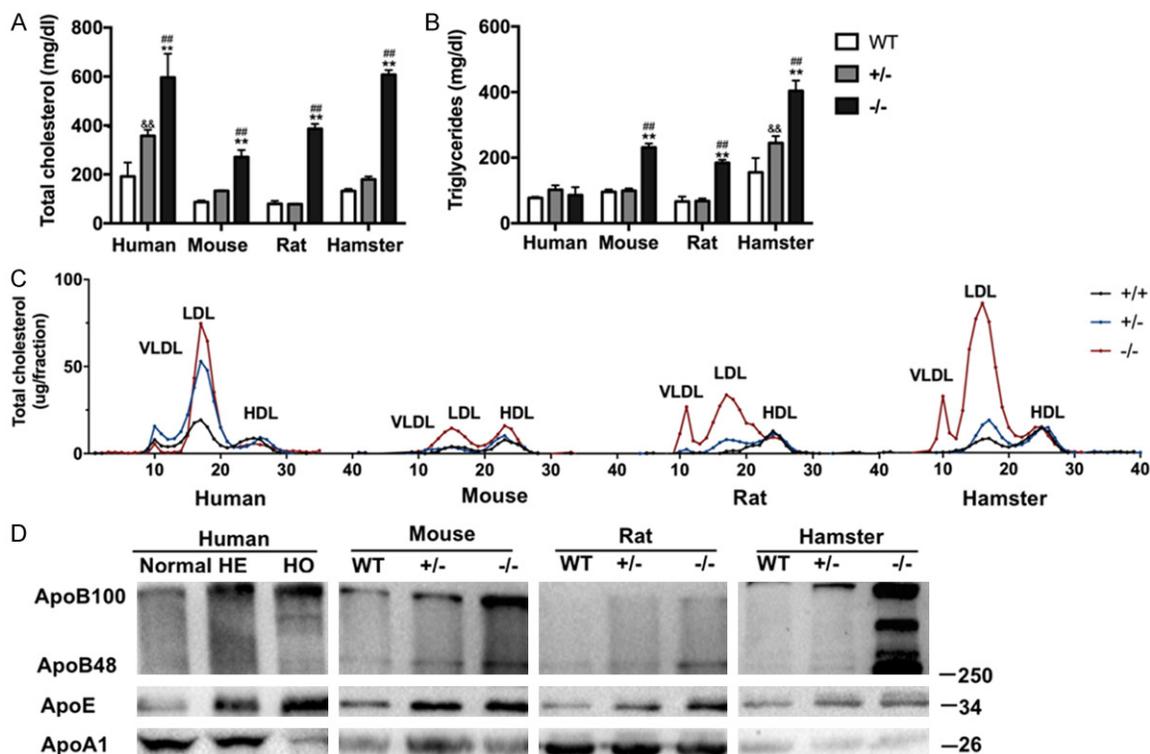
Figure 1. Plasma lipids and lipoprotein profiles in different species fed a regular chow diet. (A) Plasma total cholesterol and (B) triglycerides were measured from WT, Ldlr+/-, and Ldlr-/- rats, mice, and hamsters and in normal subjects and heterozygous and homozygous FH patients. (C) FPLC analysis of 200 μl of pooled plasma lipoprotein profiles from WT, Ldlr+/-, and Ldlr-/- rats, mice, and hamsters and FH patients. (D) Western blot analysis of plasma ApoB, ApoE and ApoA1 levels from WT, Ldlr+/-, and Ldlr-/- rats, mice, and hamsters and FH patients. Data are shown as mean ± SEM. n=3-6 per group. Significance was determined by two-way analysis of variance. *P<0.05, **P<0.01, &&P<0.01 VS WT, #P<0.05, ##P<0.01 vs Ldlr+/-. WT: wild type, Ldlr+/-: heterozygous of low-density lipoprotein receptor, Ldlr-/-: low-density lipoprotein receptor knockout.

at 608±18 mg/dL, similar to that in HoFH patients. However, cholesterol levels were moderately increased in Ldlr-/- rats and mice and were close to HeFH patients (357±24 mg/dL). Interestingly, plasma TG levels were significantly increased in all Ldlr-/- animals, with the highest level in hamsters, but there were no significant differences among the three human genotypes (**Figure 1A** and **1B**). Next, we studied plasma lipoprotein profiles in different species. As shown in **Figure 1C**, HoFH patients and Ldlr-/- hamsters show dominant LDL-C in a gene dosage-dependent manner, whereas Ldlr-/- mice showed high cholesterol content in LDL and HDL fractions, and Ldlr-/- rats exhibited high levels of both very low-density lipoprotein cholesterol (VLDL-C) and LDL-C. Moreover, unlike in humans and hamsters, HDL was found a dominant lipoprotein in both Ldlr+/- mice and rats. Since apolipoproteins are key structural and functional components of lipoproteins, it is important to characterize plasma apolipoprotein levels in these species. Our immunoblot data revealed that ApoB and ApoE were significantly increased in hamsters, mice, rats, and FH patients with a gene dosage-dependent effect. However, ApoA1 levels were markedly reduced in HoFH patients but unaltered in Ldlr-/- animals (**Figure 1D**). Collectively, these findings from lipid studies in chow diet-fed animals suggest that Ldlr KO hamsters better replicate the lipid metabolism phenotype in FH.

Analysis of HCHF diet-induced hyperlipidemia in mice, rats, and hamsters with Ldlr deficiency

To investigate the responses to diet-induced hyperlipidemia in different Ldlr KO species, WT, Ldlr+/-, Ldlr-/- animals were divided into nine groups. Animals were challenged with an HCHF diet containing 0.5% cholesterol and 15% fat for 12 weeks, and plasma TC and TG were mea-
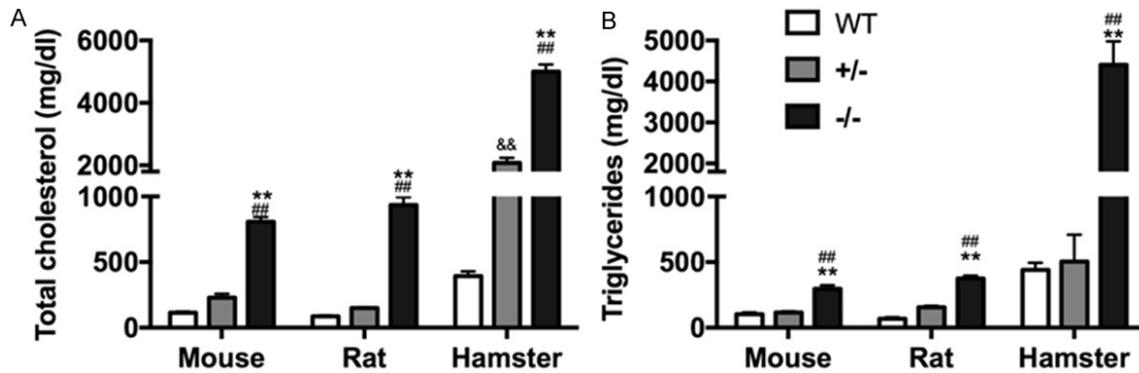
Figure 2. Plasma lipids in different species upon 12-week HCHF diet feeding. (A) Plasma TC and (B) TG from WT, Ldlr+/- and Ldlr-/- rats, mice, and hamsters on an HCHF diet for 12 weeks (n=6 per group). Data are shown as mean ± SEM. **P<0.01, &&P<0.01 VS WT, ##P<0.01 vs Ldlr+/-. WT: wild type, Ldlr+/-: heterozygous of low-density lipoprotein receptor, Ldlr-/-: low-density lipoprotein receptor knockout, HCHF: high-cholesterol/high-fat.

sured at different time points. Compared to mice and rats, HCHF-fed hamsters developed severe hypercholesterolemia in both the Ldlr+/- (2081±161 mg/dL) and Ldlr-/- (4997±233 mg/dL) groups, but the cholesterol levels were only significantly increased in Ldlr-/- mice and rats (not Ldlr+/-). Moreover, the levels were still lower than that observed in Ldlr+/- hamsters, suggesting that mice and rats are resistant to diet-induced hyperlipidemia if they carry a single copy of *Ldlr* gene. Interestingly, WT hamsters showed higher TG levels compared to mice and rats, and Ldlr-/- hamsters displayed hypertriglyceridemia (HTG) after 12-week HCHF diet consumption, while TG was only mildly increased in Ldlr-/- mice and rats (**Figure 2**). Since hyperlipidemia is highly associated with non-alcohol fatty liver disease (NAFLD), we also investigated the effects of an HCHF diet on NAFLD in different species. As shown in Figure S1, HE staining showed lipid accumulation in both Ldlr+/- and Ldlr-/- hamsters, which also exhibited hepatic fibrosis on Sirius red staining with increased contents of TC and TG. This indicates that Ldlr KO hamsters are sensitive to diet-induced hyperlipidemia and fatty liver, which were not observed in mice and rats. Our data demonstrate that hamsters, especially with those lacking one or both copies of the *Ldlr* gene, are useful for studying diet-induced combined hyperlipidemia.

HCHF diet-induced atherosclerosis in different rodent models

Atherosclerosis is one of the consequences of hypercholesterolemia. We studied atheroscle-

rosis in different species fed an HCHF diet for 12 weeks. After treatment, we collected the whole aortas for ORO staining (**Figure 3A**). WT and Ldlr+/- mice and rats had no atherosclerotic plaques, and Ldlr-/- rats showed far fewer atherosclerotic lesions (4.4%) than Ldlr-/- mice (21%). By contrast, WT hamsters had visible lesions (3.2%), and Ldlr+/- and Ldlr-/- hamsters exhibited more severe atherosclerotic lesions (14% and 33%, respectively, compared to the corresponding mice and rats), indicating that Ldlr KO hamsters are more sensitive to diet-induced atherosclerosis (**Figure 3B**). Further analysis revealed that the Ldlr-/- mice largely developed atherosclerosis in the aortic arch; however, atherosclerotic lesions in Ldlr-/- hamsters were in the aortic arch, and thoracic and abdominal aortas, a distribution pattern consistent with FH patients (**Figure 3C**). Similar to the observations in whole aortas, data from cross-sections showed that there were no atherosclerotic lesions in WT and Ldlr+/- mice and rats (**Figure 3D**). Notably, HCHF diet-fed hamsters exhibited accelerated atherosclerotic development in the aortic roots with a gene dosage-dependent effect (3.4×10^4 μm², 1.0×10^5 μm², and 2.9×10^5 μm², respectively). Interestingly, compared to Ldlr-/- hamsters, Ldlr-/- mice also showed comparable plaque sizes in aortic roots (4.2×10^5 μm²), but not in thoracic or abdominal segments (**Figure 3E**). Consistently, the immunohistochemical results suggested that CD68 and VCAM1, two key components of atherosclerotic lesions, were highly associated with lesion size (Figure S2).
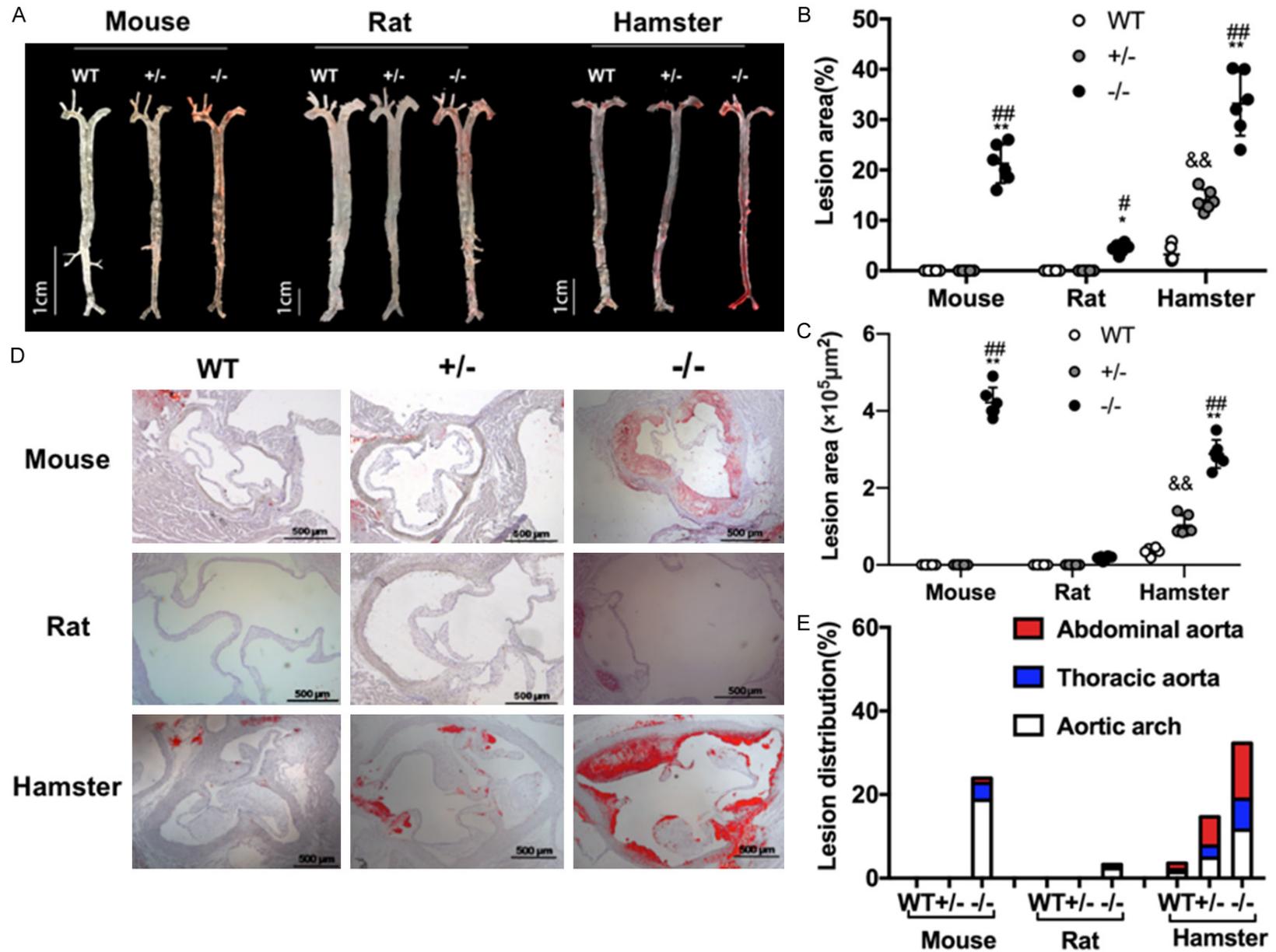
Figure 3. The characteristics of HCHF diet-induced atherosclerosis in different species. (A) Representative images of Oil Red O stained en face aortas from WT, Ldlr KO+/-, and Ldlr KO-/- rats, mice, and hamsters with 12-week HCHF diet treatment. (B) Quantification of atherosclerotic lesion sizes in the whole aortas from (A). (C) Analysis of the plaque distribution in WT, Ldlr KO+/-, and Ldlr KO-/- rats, mice, and hamsters after a 12-week HCHF diet. Aortic arch: aortic root to below the left subclavian. Thoracic aorta: the region between the end of the arch and the last intercostal branch. Abdominal aorta: the region between the end of the thoracic aorta segment and the iliac bifurcation. (D) Representative images of aortic root sections with Oil Red O staining from WT, Ldlr KO+/-, and Ldlr KO-/- rats, mice, and hamsters with 12-week HCHF diet treatment. Scale bar =500 μm. (E) Quantification of lesion areas in aortic roots. Data are expressed as mean ± SEM. n=6 per group. *$P<0.05$, **$P<0.01$, &&$P<0.01$ VS WT, #$P<0.05$, ##$P<0.01$ vs Ldlr+/-. WT: wild type, Ldlr+/-: heterozygous of low-density lipoprotein receptor, Ldlr-/-: low-density lipoprotein receptor knockout, HCHF: high-cholesterol/high-fat.

Coronary atherosclerosis induced by an HCHF diet

Coronary atherosclerosis is a feature of FH. However, atherosclerotic plaques in en face and aortic roots are always used to evaluate the atherosclerosis under dyslipidemic conditions in experimental animal studies because mice seldom exhibit coronary lesions. To fully understand coronary atherosclerosis pathogenesis in different rodents with Ldlr deficiency after 12 weeks of an HCHF diet, we scored occlusion of coronary atherosclerosis in ORO-stained sections. As shown in **Figure 4**, rats did not show coronary atherosclerosis, and only 22% of coronary arteries had atherosclerotic plaques in Ldlr-/- mice without >50% occlusion. In contrast to rats and mice, 48% of coronary arteries showed atherosclerotic lesions in Ldlr+/- hamsters, and Ldlr-/- hamsters had the highest proportion of coronary atherosclerosis (82%), with 8% of coronary arteries having >50% occlusion. Collectively, these findings suggest that hamsters are more susceptible to coronary atherosclerosis induced by an HCHF diet and may provide invaluable insight into human atherosclerosis.

Discussion

FH is largely attributed to the loss-of-function mutations in the human *Ldlr* gene, leading to impaired removal of LDL-C from the circulation, followed by elevated plasma TC and LDL-C levels and premature atherosclerotic CVD [1, 2, 21, 22]. Although Ldlr KO mice have been extensively used to study FH, a growing body of evidence indicates that homozygous Ldlr KO mice only show moderately increased LDL-C and do not develop atherosclerosis without other gene manipulations or environmental interventions [3, 23]. This suggests that better rodent animal models are needed for FH stud-

ies. Rats and hamsters with CRISPR/Cas9-mediated deletion of the *Ldlr* gene were recently generated, providing an opportunity to compare the roles of Ldlr in FH in different species. The present work is the first interspecies study to fully characterize lipoprotein metabolism and atherosclerotic CVD in Ldlr KO mice, rats, and hamsters and compare findings with FH patients. In contrast to mice and rats, but like FH patients, Ldlr KO hamsters exhibited markedly increased plasma TC with LDLs as the dominant lipoproteins in a gene dosage-dependent manner, even when fed a regular chow diet. After 12 weeks of consuming an HCHF diet, Ldlr KO rats did not develop atherosclerosis, but Ldlr KO mice and hamsters showed evidence of diet-induced atherosclerosis. However, only HCHF-fed Ldlr KO hamsters displayed coronary and abdominal atherosclerosis, which has been reported in humans. These meaningful data demonstrate that Ldlr KO hamsters, including heterozygotes, could be an invaluable model to investigate LDLR-mediated lipid metabolism and the pathological consequences of dysfunctional LDLR regulation for translational study in human disease.

Ldlr gene mutations in FH patients significantly affect plasma TC with a gene dosage-dependent effect, leading to moderate and severe hypercholesterolemia in heterozygous and homozygous populations, respectively. Unlike FH patients, deleting one copy of the *Ldlr* gene did not influence plasma TC in mice and rats fed a regular chow diet treatment, and the TC levels were only slightly increased in homozygotes. However, Ldlr+/- and Ldlr-/- hamsters displayed moderate and marked increases in plasma cholesterols, respectively. This was especially true for LDL-C, which is also the case in FH patients. It should be noted that Apobec-1, an enzyme required for ApoB editing, is expressed in the liver and intestine of mice and rats.
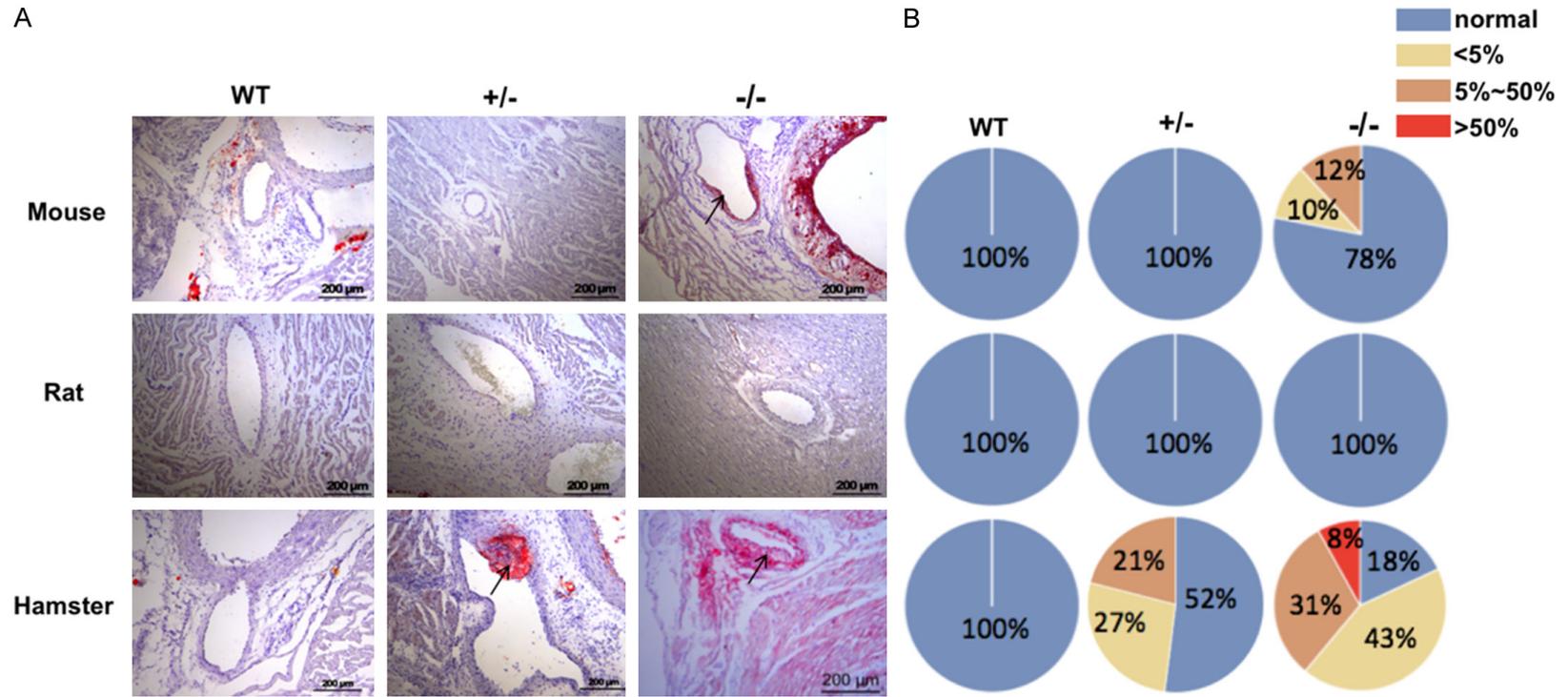
Figure 4. Analysis of coronary atherosclerosis in animals after 12-week HCHF diet feeding. (A) Representative images of coronary arteries stained with ORO from WT, Ldlr+/-, and Ldlr-/- mice, rats, and hamsters with 12-week HCHF diet treatment. (B) Semi-quantification of coronary atherosclerosis in each group from (A). Arrows indicate atherosclerotic lesions in the coronary arteries. WT: wild type, Ldlr+/-: heterozygous of low-density lipoprotein receptor, Ldlr-/-: low-density lipoprotein receptor knockout, HCHF: high-cholesterol/high-fat.

Mouse and rat VLDL/IDL particles contain both ApoB100 and -48. Since ApoB48-containing lipoproteins possess a high fractional catabolic rate and HDL-C cannot be transferred to VLDL due to a lack of CETP, HDL is the major lipoprotein in mice and rats. On an HCHF diet, these dietary lipids are assembled into very large lipoproteins and are still effectively removed from circulation in Ldlr+/- mice and rats. In contrast, there is no hepatic Apobec-1 expression in hamsters and humans, but there are high levels of CETP activity [24, 25], both of which contribute to the stability of large lipoprotein particles in plasma. In addition, reduced LDLR protein in the liver is insufficient to clear accumulated lipoproteins in Ldlr+/- hamsters, predisposing them to diet-induced hyperlipidemia. Therefore, Ldlr+/- hamsters could serve as an ideal model to study the molecular mechanisms involved in LDLR regulation and assess drug efficacy.

It is important to notice that compared to other species, complete loss of the *Ldlr* gene in hamsters caused increased baseline TG levels and exacerbated HTG with severe hypercholesterolemia, and these animals developed combined hyperlipidemia in response to a 12-week HCHF diet. However, this combination is rare in FH patients, and whether HTG can be induced is unknown because an HCHF diet intervention could not be considered for clinical FH patients. We previously demonstrated that Ldlr deficiency did not alter lipoprotein lipase (LPL) enzyme activity in hamsters, which is required to clear plasma TG-rich large lipoproteins. Moreover, chylomicron remnants from LPL-mediated lipolysis accumulated in Ldlr-/- mice, suggesting that the LDLR pathway is critical for the removal of TG as well as cholesterol [26]. Our western blot results further confirmed that ApoB100/48 and ApoE, two key components of large lipoproteins, were accumulated in all Ldlr mutant species in a gene dose-dependent manner. Since hamsters possess the highest CETP activity and CETP inhibitors have been reported to lower plasma TG, it will be interesting to test the effect of CETP inhibition on TG metabolism in our Ldlr KO hamsters.

Atherosclerotic coronary heart disease (ASCHD) is one of the features of FH [27-29], with a mean age of onset from 45 to 55 in HeFH patients and as early as adolescence or childhood in HoFH patients. Unlike HeFH patients, Ldlr+/- mice exhibit unchanged plasma cholesterol levels compared to WT controls and do not develop atherosclerosis, indicating that they are not a good model for human atherosclerosis study. Furthermore, atherosclerotic lesions are often induced in the Ldlr-/- mice with the Paigen diet, which causes severe liver toxicity. To avoid confounding effects of this diet and investigate accelerated atherosclerotic development in different species, we placed all three species on an HCHF diet for 12 weeks and found that the atherosclerotic lesions were restricted to the aortic arch and thoracic aorta in Ldlr-/- mice, while there were no lesions in Ldlr+/- mice. Interestingly, both Ldlr+/- and Ldlr-/- hamsters showed atherosclerotic lesions in coronary arteries and whole aortas, including the thoracic and abdominal segments, with more severe lesions in whole aortas and coronary artery occlusion in Ldlr-/- hamsters. Consistent with this, previous reports propose that atherosclerosis begins as fatty streak deposits in the right coronary artery and abdominal aorta of young persons, indicating that these two sites are critical for atherosclerosis development [30, 31]. Additionally, FH patients have an atherosclerosis distribution in the carotid, thoracic, and abdominal arteries [32-34]. It was surprising that Ldlr KO rats on an HCHF diet for 12 weeks did not develop discernable atherosclerotic lesions, which is similar to the absence of this finding in Ldlr-/- rats on a Western diet (WD) for 16 weeks. However, when Ldlr-/- rats were fed a WD for 52 or 72 weeks, atherosclerotic lesions were found in the whole aortas and coronary arteries [10]. These observations suggest that Ldlr-/- rats are more resistant to diet-induced hyperlipidemia and ASCHD than Ldlr-/- hamsters. This could be an ideal rodent animal model to mimic the central features of FH.

Porcine models of Ldlr mutations recently gained attention for FH studies because the size is close to that of humans. Davis and colleagues generated homozygous Ldlr-targeted Yucatan miniature pigs showing hypercholesterolemia (<1000 mg/dL) and coronary artery disease after being fed an HCHF diet for 180 days, but no obvious atherosclerotic plaque was observed in the heterozygous pigs despite a modest increase in plasma cholesterol (>300 mg/dL), which differed from FH patients [35] and

our heterozygous hamster model. Importantly, there is high variability in the genetic backgrounds of Ldlr-targeted Yucatan miniature pigs and a long-term HCHF diet is required for atherosclerosis studies using these animals. The validity of this porcine model was questioned by Li and colleagues in a study where *Ldlr* gene was deleted in domestic pigs. The Ldlr-deficient domestic pigs on a 4-month HCHF diet showed human-like advanced coronary plaque that was attenuated by prophylactic statin treatment [36]. Unfortunately, data regarding atherosclerosis and CHD in heterozygous Ldlr-deficient domestic pigs were not presented by the authors. The unchanged plasma lipid levels in the heterozygotes suggest that domestic pigs are not an ideal animal model for FH, particularly for translational studies on HeFH.

Although data from Ldlr KO hamsters suggest that this species could replicate the major features of FH, including lipoprotein profiles with LDL-C dominance and the atherosclerotic lesion distribution, there are two important questions that need to be answered in future studies. Firstly, why do Ldlr-/- hamsters show increased VLDL-C and is this increase in VLDL-C associated with high CETP activity? Secondly, will a chronic HCHF diet (e.g., 52 weeks) exacerbate atherosclerotic development in Ldlr KO hamsters? Taken together, the results from this extensive interspecies comparison study demonstrate that Ldlr KO hamsters could provide new insight into FH and human atherosclerosis.

Acknowledgements

Disclosure of conflict of interest

None.

Address correspondence to: Xunde Xian, Department of Molecular Genetics, UT Southwestern Medical Center, Dallas 75390, Texas, USA. E-mail: xunde.xian@utsouthwestern.edu; George Liu, Institute of Cardiovascular Sciences and Key Laboratory of Molecular Cardiovascular Sciences, Ministry of Education, Peking University, Beijing 100191, China. E-mail: georgeliu@bjmu.edu.cn

References

[1] Mytilinaiou M, Kyrou I, Khan M, Grammatopoulos DK and Randeva HS. Familial hypercholesterolemia: new horizons for diagnosis and effective management. Front Pharmacol 2018; 9: 707.

[2] Ito MK and Watts GF. Challenges in the diagnosis and treatment of homozygous familial hypercholesterolemia. Drugs 2015; 75: 1715-1724.

[3] Emini Veseli B, Perrotta P, De Meyer GRA, Roth L, Van der Donckt C, Martinet W and De Meyer GRY. Animal models of atherosclerosis. Eur J Pharmacol 2017; 816: 3-13.

[4] Poledne R and Jurcikova-Novotna L. Experimental models of hyperlipoproteinemia and atherosclerosis. Physiol Res 2017; 66: 69-75.

[5] Russell JC and Proctor SD. Small animal models of cardiovascular disease: tools for the study of the roles of metabolic syndrome, dyslipidemia, and atherosclerosis. Cardiovasc Pathol 2006; 15: 318-330.

[6] Barter PJ, Brewer HB Jr, Chapman MJ, Hennekens CH, Rader DJ and Tall AR. Cholesteryl ester transfer protein: a novel target for raising HDL and inhibiting atherosclerosis. Arterioscler Thromb Vasc Biol 2003; 23: 160-167.

[7] Getz GS and Reardon CA. Diet and murine atherosclerosis. Arterioscler Thromb Vasc Biol 2006; 26: 242-249.

[8] Nishina PM, Verstuyft J and Paigen B. Synthetic low and high fat diets for the study of atherosclerosis in the mouse. J Lipid Res 1990; 31: 859-869.

[9] Wang HY, Quan C, Hu C, Xie B, Du Y, Chen L, Yang W, Yang L, Chen Q, Shen B, Hu B, Zheng Z, Zhu H, Huang X, Xu G and Chen S. A lipidomics study reveals hepatic lipid signatures associating with deficiency of the LDL receptor in a rat model. Biol Open 2016; 5: 979-986.

[10] Sithu SD, Malovichko MV, Riggs KA, Wickramasinghe NS, Winner MG, Agarwal A, Hamed-Berair RE, Kalani A, Riggs DW, Bhatnagar A and Srivastava S. Atherogenesis and metabolic dysregulation in LDL receptor-knockout rats. JCI Insight 2017; 2.

[11] Dorfman SE, Smith DE, Osgood DP and Lichtenstein AH. Study of diet-induced changes in lipoprotein metabolism in two strains of Golden-Syrian hamsters. J Nutr 2003; 133: 4183-4188.

[12] Nistor A, Bulla A, Filip DA and Radu A. The hyperlipidemic hamster as a model of experimental atherosclerosis. Atherosclerosis 1987; 68: 159-173.

[13] Remillard P, Shen G, Milne R and Maheux P. Induction of cholesteryl ester transfer protein in adipose tissue and plasma of the fructose-fed hamster. Life Sci 2001; 69: 677-687.

[14] Guo X, Gao M, Wang Y, Lin X, Yang L, Cong N, An X, Wang F, Qu K, Yu L, Wang Y, Wang J, Zhu H, Xian X and Liu G. LDL receptor gene-ablated hamsters: a rodent model of familial hypercholesterolemia with dominant inheritance and diet-induced coronary atherosclerosis. EBioMedicine 2018; 27: 214-224.

[15] Wu WF, Sun LY, Pan XD, Yang SW and Wang LY. Use of targeted exome sequencing in genetic diagnosis of Chinese familial hypercholesterolemia. PLoS One 2014; 9: e94697.

[16] Jiang L, Sun LY, Pan XD, Chen PP, Tang L, Wang W, Zhao LM, Yang SW and Wang LY. Characterization of the unique Chinese W483X mutation in the low-density lipoprotein-receptor gene in young patients with homozygous familial hypercholesterolemia. J Clin Lipidol 2016; 10: 538-546.

[17] Xian X, Ding Y, Dieckmann M, Zhou L, Plattner F, Liu M, Parks JS, Hammer RE, Boucher P, Tsai S and Herz J. LRP1 integrates murine macrophage cholesterol homeostasis and inflammatory responses in atherosclerosis. Elife 2017; 6.

[18] Bligh EG and Dyer WJ. A rapid method of total lipid extraction and purification. Can J Biochem Physiol 1959; 37: 911-917.

[19] Liu XJ, Wu XY, Wang H, Wang SX, Kong W, Zhang L, Liu G and Huang W. Renal injury in Seipin-deficient lipodystrophic mice and its reversal by adipose tissue transplantation or leptin administration alone: adipose tissue-kidney crosstalk. FASEB J 2018; 32: 5550-5562.

[20] Miyaoka Y, Jin D, Tashiro K, Komeda K, Masubuchi S, Hirokawa F, Hayashi M, Takai S and Uchiyama K. Chymase inhibitor prevents the development and progression of non-alcoholic steatohepatitis in rats fed a high-fat and high-cholesterol diet. J Pharmacol Sci 2017; 134: 139-146.

[21] Hartgers ML, Ray KK and Hovingh GK. New approaches in detection and treatment of familial hypercholesterolemia. Curr Cardiol Rep 2015; 17: 109.

[22] Baum SJ, Soifer D and Duell PB. Emerging treatments for heterozygous and homozygous familial hypercholesterolemia. Rev Cardiovasc Med 2016; 17: 17-25.

[23] Getz GS and Reardon CA. Do the Apoe(-/-) and Ldlr(-/-) mice yield the same insight on atherogenesis? Arterioscler Thromb Vasc Biol 2016; 36: 1734-1741.

[24] Greeve J, Axelos D, Welker S, Schipper M and Greten H. Distinct promoters induce APOBEC-1 expression in rat liver and intestine. Arterioscler Thromb Vasc Biol 1998; 18: 1079-1092.

[25] Reaves SK, Wu JY, Wu Y, Fanzo JC, Wang YR, Lei PP and Lei KY. Regulation of intestinal apolipoprotein B mRNA editing levels by a zinc-deficient diet and cDNA cloning of editing protein in hamsters. J Nutr 2000; 130: 2166-2173.

[26] Ishibashi S, Perrey S, Chen Z, Osuga J, Shimada M, Ohashi K, Harada K, Yazaki Y and Yamada N. Role of the low density lipoprotein (LDL) receptor pathway in the metabolism of chylomicron remnants. A quantitative study in knockout mice lacking the LDL receptor, apolipoprotein E, or both. J Biol Chem 1996; 271: 22422-22427.

[27] Stone NJ, Fredrickson DS, Verter J and Levy RI. Coronary-artery disease in 116 kindred with familial type-Ii hyperlipoproteinemia. Circulation 1974; 49: 476-488.

[28] Humphries SE, Cooper JA, Seed M, Capps N, Durrington PN, Jones B, McDowell IFW, Soran H, Neil HAW; Simon Broome Familial Hyperlipidaemia Register Group. Coronary heart disease mortality in treated familial hypercholesterolaemia: update of the UK Simon Broome FH register. Atherosclerosis 2018; 274: 41-46.

[29] Marks D, Thorogood M, Neil HA and Humphries SE. A review on the diagnosis, natural history, and treatment of familial hypercholesterolaemia. Atherosclerosis 2003; 168: 1-14.

[30] McGill HC, McMahan CA, Herderick EE, Malcom GT, Tracy RE, Strong JP and Ather PD. Origin of atherosclerosis in childhood and adolescence. Am J Clin Nutr 2000; 72 Suppl: 1307S-1315S.

[31] McGill HC Jr, McMahan CA, Herderick EE, Tracy RE, Malcom GT, Zieske AW and Strong JP. Effects of coronary heart disease risk factors on atherosclerosis of selected regions of the aorta and right coronary artery. PDAY research group. Pathobiological determinants of atherosclerosis in youth. Arterioscler Thromb Vasc Biol 2000; 20: 836-845.

[32] Roberts WC, Won VS, Weissenborn MR, Khalid A and Lima B. Massive diffuse calcification of the ascending aorta and minimal focal calcification of the abdominal aorta in heterozygous familial hypercholesterolemia. Am J Cardiol 2016; 117: 1381-1385.

[33] Ribeiro P, Shapiro LM, Gonzalez A, Thompson GR and Oakley CM. Cross sectional echocardiographic assessment of the aortic root and coronary ostial stenosis in familial hypercholesterolaemia. Br Heart J 1983; 50: 432-437.

[34] Aggeli C, Kazazaki C, Felekos I, Roussakis G, Lagoudakou S, Skoumas J, Toutouzas K, Tousoulis D, Pitsavos C and Stefanadis C. Role of real time-3D transesophageal echocardiography in evaluating the atheromatous burden of

thoracic aorta in patients with heterozygous familial hypercholesterolemia: comparison with 2D transesophageal study. Int J Cardiol 2011; 150: 92-93.

[35] Davis BT, Wang XJ, Rohret JA, Struzynski JT, Merricks EP, Bellinger DA, Rohret FA, Nichols TC and Rogers CS. Targeted disruption of LDLR causes hypercholesterolemia and atherosclerosis in Yucatan miniature pigs. PLoS One 2014; 9: e93457.

[36] Li YX, Fuchimoto D, Sudo M, Haruta H, Lin QF, Takayama T, Morita S, Nochi T, Suzuki S, Sembon S, Nakai M, Kojima M, Iwamoto M, Hashimoto M, Yoda S, Kunimoto S, Hiro T, Matsumoto T, Mitsumata M, Sugitani M, Saito S, Hirayama A and Onishi A. Development of human-like advanced coronary plaques in low-density lipoprotein receptor knockout pigs and justification for statin treatment before formation of atherosclerotic plaques. J Am Heart Assoc 2016; 5: e002779.
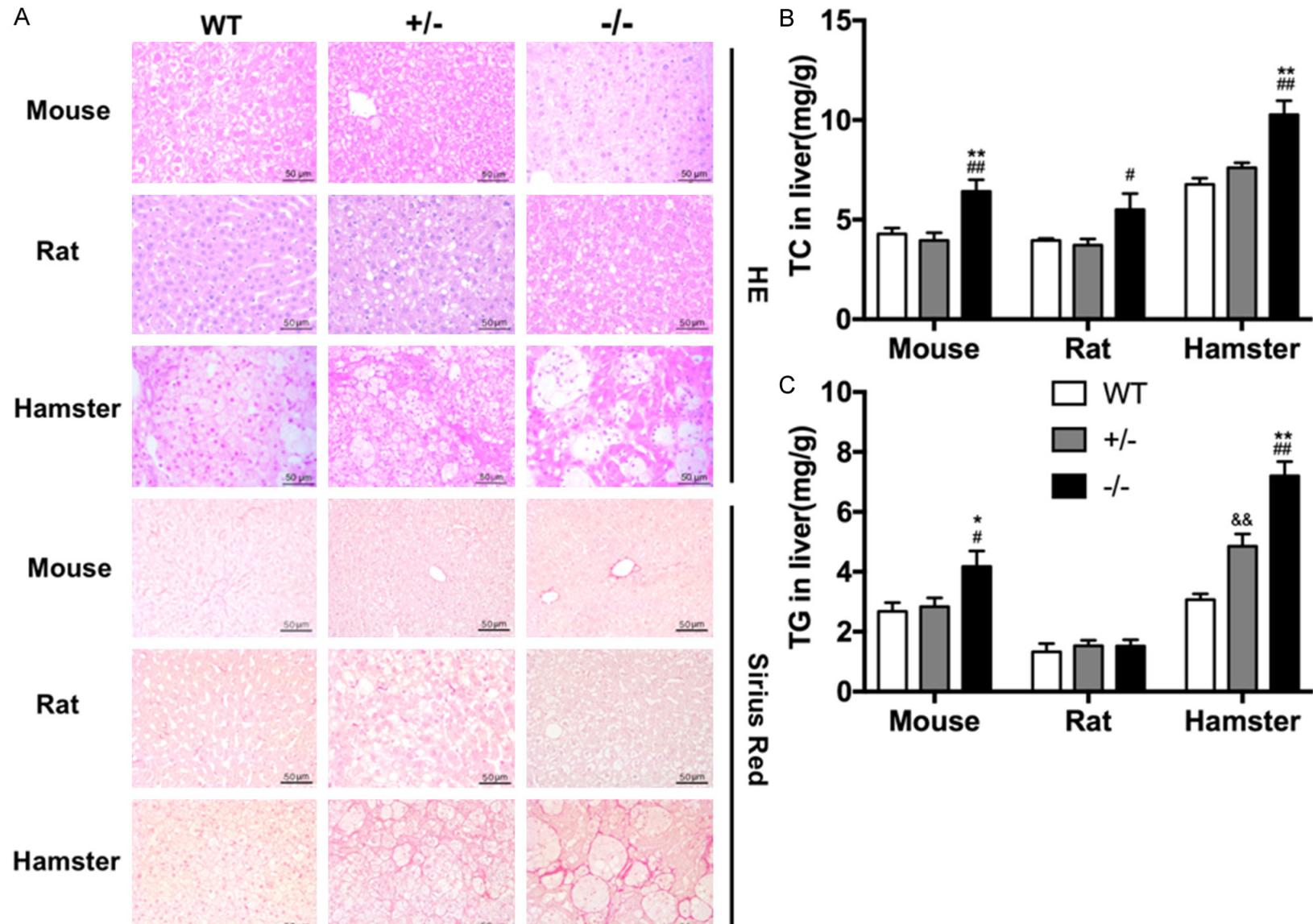
Figure S1. An HCHF diet induced NAFLD in hamsters, but not in mice or rats. (A) Representative staining with HE (upper panel) and Sirius red (lower panel) in liver tissue from WT, Ldlr KO+/-, and Ldlr KO-/- rats, mice, and hamsters with 12-week HCHF diet treatment. Scale bar =50 μm. (B, C) Hepatic TC (B) and TG (C) contents were measured and normalized to liver weight (n=4/group). Data are shown as mean ± SEM. *P<0.05, **P<0.01, &&P<0.01 VS WT, #P<0.05, ##P<0.01 vs Ldlr+/-. WT: wild type, Ldlr+/-: heterozygous of low-density lipoprotein receptor, Ldlr-/-: low-density lipoprotein receptor knockout, HCHF: high-cholesterol/high-fat.
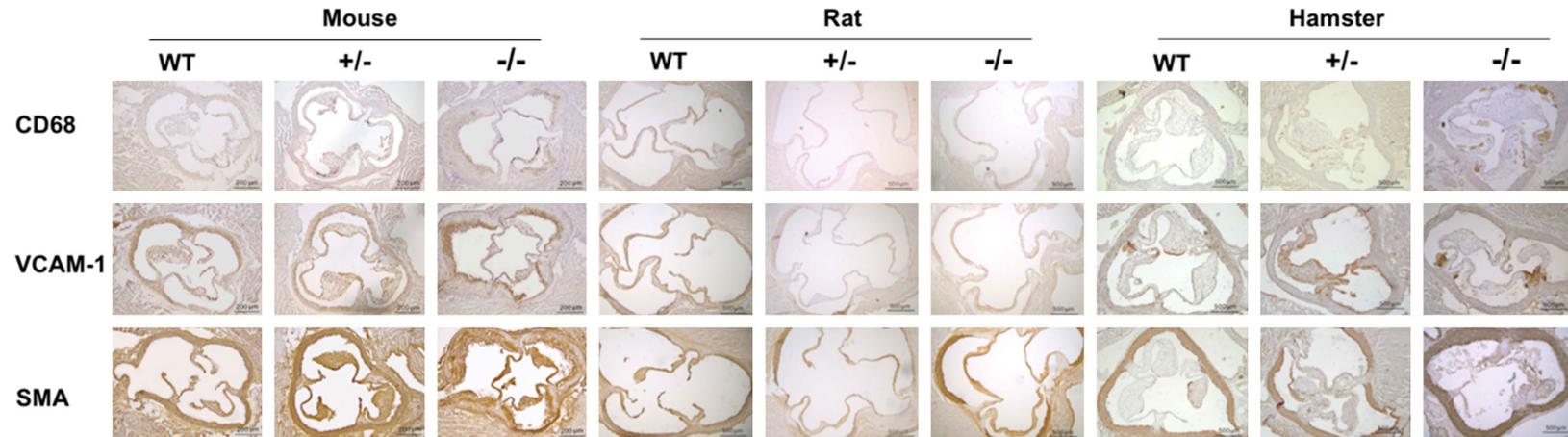
Figure S2. Analysis of atherosclerotic plaque components in animals after 12-week HCHF diet feeding. Atherosclerotic lesion components in WT, Ldlr KO+/-, and Ldlr KO-/- rats, mice, and hamsters on a 12-week HCHF diet were analyzed with immunohistochemical staining using antibodies against CD68, VCAM-1, and α-SMA. Representative images of aortic root sections stained for CD68 (upper panel), VCAM-1 (middle panel), and α-SMA (lower panel). Scale bar =200/500 μm. WT: wild type, Ldlr+/-: heterozygous of low-density lipoprotein receptor, Ldlr-/-: low-density lipoprotein receptor knockout, HCHF: high-cholesterol/high-fat.